JOURNAL OF GEOPHYSICAL RESEARCH, VOL. 107, NO. A11, 1339, doi:10.1029/2001JA009211, 2002

A new model of the location of the plasmapause: CRRES results

Mark B. Moldwin
Department of Earth and Space Sciences, University of California, Los Angeles, Los Angeles, California, USA

L. Downward, H. K. Rassoul and R. Amin
Department of Physics and Space Sciences, Florida Institute of Technology, Melbourne, Florida, USA

R. R. Anderson
University of Iowa, Iowa City, Iowa, USA

Received 12 December 2001; revised 26 April 2002; accepted 15 May 2002; published 2 November 2002.

[1] A new empirical model of the plasmapause location has been developed using density data from the plasma wave receiver onboard the CRRES spacecraft for nearly 1000 orbits. The "plasmapause" is identified here as the innermost sharp gradient in density (change of a factor of 5 in <0.5 L). Such a sharp gradient was observed on 73% of the CRRES inbound and outbound orbits that returned data. The plasmapause location is expressed as a linear function of *Kp* (previous 12 hour maximum) and local time. The model gives the linear best fit location of the plasmapause as well as the standard deviations of the model parameters. We found a slight noon-midnight asymmetry with the plasmapause located on average an L shell farther from the Earth at midnight than in the noon sector. This is in the opposite sense to the noon-midnight asymmetry found previously. Significant variability (with standard deviations up to +/− 1 L shell) in the plasmapause location is seen and suggests that though the mean plasmapause is roughly circular, the instantaneous plasmapause has significant time variable localized structure at all local times but most especially in the duskside sector. *INDEX TERMS:* 2730 Magnetospheric Physics: Magnetosphere—inner; 2740 Magnetospheric Physics: Magnetospheric configuration and dynamics; 2736 Magnetospheric Physics: Magnetosphere/ionosphere interactions; 2768 Magnetospheric Physics: Plasmasphere; *KEYWORDS:* plasmasphere, plasmapause, inner magnetosphere

Citation: Moldwin, M. B., L. Downward, H. K. Rassoul, R. Amin, and R. R. Anderson, A new model of the location of the plasmapause: CRRES results, *J. Geophys. Res.*, *107*(A11), 1339, doi:10.1029/2001JA009211, 2002.

1. Introduction

[2] The plasmasphere plays a critical role in modulating the fluxes of energetic particles [e.g., *Kozyra et al.*, 1995], strongly influences the propagation of ULF waves [e.g., *Webb and Orr*, 1975a, 1975b; *Takahashi and Anderson*, 1992], influences the plasma properties of the inner magnetosphere through particle-particle and wave-particle interactions [e.g., *Young et al.*, 1981; *Thorne and Horne*, 1992; *Wilson et al.*, 1992; *Gary et al.*, 1994], and contributes to populating the low-latitude boundary layer and plasma sheet [e.g., *Elphic et al.*, 1997; *Borovsky et al.*, 1997]. The location of the plasmapause is therefore a fundamental magnetospheric parameter that influences the propagation of mass and energy in the inner magnetosphere. The location of the plasmapause has been estimated theoretically by examining the location of the last-closed equipotential around the Earth due to the combination of the corotation and convection electric fields [e.g., *Nishida*, 1967]. This has been done for a variety of empirical convection electric field models [e.g., *Lemaire*, 1976; *Doe et al.*, 1992; *Maynard et al.*, 1995; *Elphic et al.*, 1997; *Lambour et al.*, 1997]. However, this approach does not lead to physically meaningful results since we do not have a good model of the subauroral ionospheric convection electric field [e.g., *Lemaire and Gringauz*, 1998]. Empirical plasmapause location models have also been calculated by examining both ground-based whistler and in situ measurements [e.g., *Chappell et al.*, 1970, 1971; *Maynard and Grebowsky*, 1977; *Horwitz et al.*, 1986; *Carpenter and Anderson*, 1992].

[3] These models find that the plasmapause slowly grows with decreasing geomagnetic activity and rapidly shrinks owing to enhanced convection activity. In addition, the theoretical models and all global empirical models predict a bulge in the dusk sector that rotates toward noon with increasing geomagnetic activity. The bulge and its behavior have also been inferred from geosynchronous orbit observations [e.g., *Higel and Wu*, 1984; *Moldwin et al.*, 1994]. However, this bulge is not seen in the data set used in *Carpenter and Anderson*'s [1992] empirical model that examined the innermost sharp density gradient location, though dense plasmaspheric plasma is often observed "outside" the main plasmasphere in the dusk region [e.g., *Carpenter and Anderson*, 1992] and bulge observations

0148-0227/02/2001JA009211

are inferred from individual spacecraft orbits [e.g., *Carpenter et al.*, 1993].

[4] These models describe the location of the plasmapause as a function of geomagnetic activity (most often parameterized by *Kp* or some *Kp* history measure). *Carpenter and Anderson* [1992] found that the plasmapause in the 0000–1500 LT sector is described by

$$\mathrm{Lpp} = 5.6 - 0.46Kp_{\max} \quad (1)$$

(where $Kp_{\max}$ is the maximum *Kp* observed in the previous 24 hours with a few caveats to attempt to account for a delay in response to changing geomagnetic activity levels for dayside plasmapause observations). This is probably the widest-used plasmapause location model [see *Gallagher et al.*, 2000] and was based on 208 ISEE 1 plasmapause crossings. No dependence on local time was found, though the dusk sector (1500–0000 LT) was not included in the empirical relationship given in equation (1).

[5] The CRRES satellite was launched in the early 1990s into a geosynchronous transfer orbit and made in situ measurements of the electron number density with the plasma wave receiver [*Anderson et al.*, 1992]. The entire CRRES database of over 1000 orbits has been examined for sharp density gradients indicative of the plasmapause. This database has a factor of 5 more plasmapause locations than the *Carpenter and Anderson* [1992] ISEE 1 database and allows us to reexamine the local time and geomagnetic activity behavior of the location of the plasmapause. This study presents a new empirical plasmapause location model that is both continuous in local time and gives a quantitative measure of the variability of the plasmapause location for a given geomagnetic activity level. This model can be incorporated into numerical inner magnetospheric models and can contribute to understanding the global plasmaspheric images now being produced by the IMAGE mission.

2. Methodology

[6] The CRRES density database was examined orbit by orbit for sharp density drops indicative of the plasmapause. This was done both visually and with a computer algorithm that located the innermost sharp density gradient of at least a factor of 5 within a radial distance of 0.5 L. This is the same selection criterion used by *Carpenter and Anderson* [1992]. The use of this criterion creates a database of "sharp" plasmapauses that are often indicative of newly formed plasmapause. However, there are examples of multiple consecutive orbits observing essentially the same plasmapause during steady geomagnetic conditions, indicating that sharp plasmapause boundaries are often long-lived. Note that the criteria for "sharp" boundaries using the quantitative criteria of this study may bias the selection to recently formed plasmapause. This caveat may be important in the dayside results discussed in section 4. The visual and computer databases were compared in order to select a "clean" plasmapause database. The plasmapause often has significant density structure, and therefore the exact location can be difficult to determine [e.g., *LeDocq et al.*, 1994; *Moldwin et al*., 1995]. In addition, density cavities are often observed within the main plasmasphere, and careful identification of these features was needed to consistently select the plasmapause [e.g., *Carpenter et al.*, 2000]. Figure 1 shows four different CRRES orbit plots showing the variety of plasmapause observations routinely seen in the CRRES database.

[7] Clean and sharp "classic" plasmapauses (Figure 1a) are a minority of the CRRES orbits (154 of the 969 identified plasmapauses or 16%). Plasmapause observations with significant structure (Figure 1b) or density cavities (Figure 1c) are more common. A small percentage of CRRES orbits did not observe a plasmapause at all but instead remained inside an extended plasmasphere out to apogee (Figure 1d). These last types of orbits were excluded from the database, though they are discussed in more detail in section 4. Another difficulty, though impacting only a small fraction of the orbits, were plasmapauses located inside of an L of 2. Owing to the upper frequency limit of 400 kHz (and hence maximum density limit of $\sim$2000 cm^{-3}) of the sweep frequency receiver, readings within L of 2 were often "saturated." Therefore even though large density drops were occasionally observed, they would often not meet the factor of 5 density drop.

[8] In roughly 40% of the orbits, particularly in the 1200–2000 LT sector, significant density is observed beyond the innermost large density gradient, which we identify as the plasmapause (e.g., Figure 1b). However, in many of these examples the outer density structure does not meet our steep density gradient criteria for the plasmapause. The structure beyond the plasmapause has been interpreted as plasma tails or plumes of plasmaspheric plasma convecting Sunward. In addition, this plasma may be from flux tubes on fairly recently (12–48 hours earlier) closed or corotating drift paths that are partially refilled during the recovery after a disturbed interval. In this case, if the inner density steep gradient has a lifetime comparable to the refilling time, then our results are more indicative of the earlier disturbed conditions than to the current recovery conditions.

3. Model Results

3.1. Plasmapause Locations

[9] An identifiable plasmapause was observed on 73% of the inbound and outbound trajectories (969 of the 1328 inbound and outbound orbits) that had data. Of the 2012 possible plasmapause crossings (two per orbit) there were data for 1328 (68% orbital coverage). In several of the orbits there are data for one leg of the trajectory but data gaps during the other half of the orbit, and hence we divide each orbit into inbound and outbound to get a more accurate description of the data coverage with regard to the number of plasmapauses identified. Figure 2 shows the location of the plasmapauses identified in this study overlaid on a plot of data occurrence duration frequency as a function of LT and L shell. Note that owing to the 18° inclination of the CRRES spacecraft, sampling out to L shells beyond 7 was possible. The gap in the orbital coverage around noon at high L shells was due to the failure of the spacecraft prior to precessing completely around the Earth. Gaps in data coverage near midnight at middle radial distances are due to temporary communication failures.

[10] There are several reasons why on 359 of the possible inbound and outbound trajectories no plasmapause was detected. For many orbits (44 of the total number of

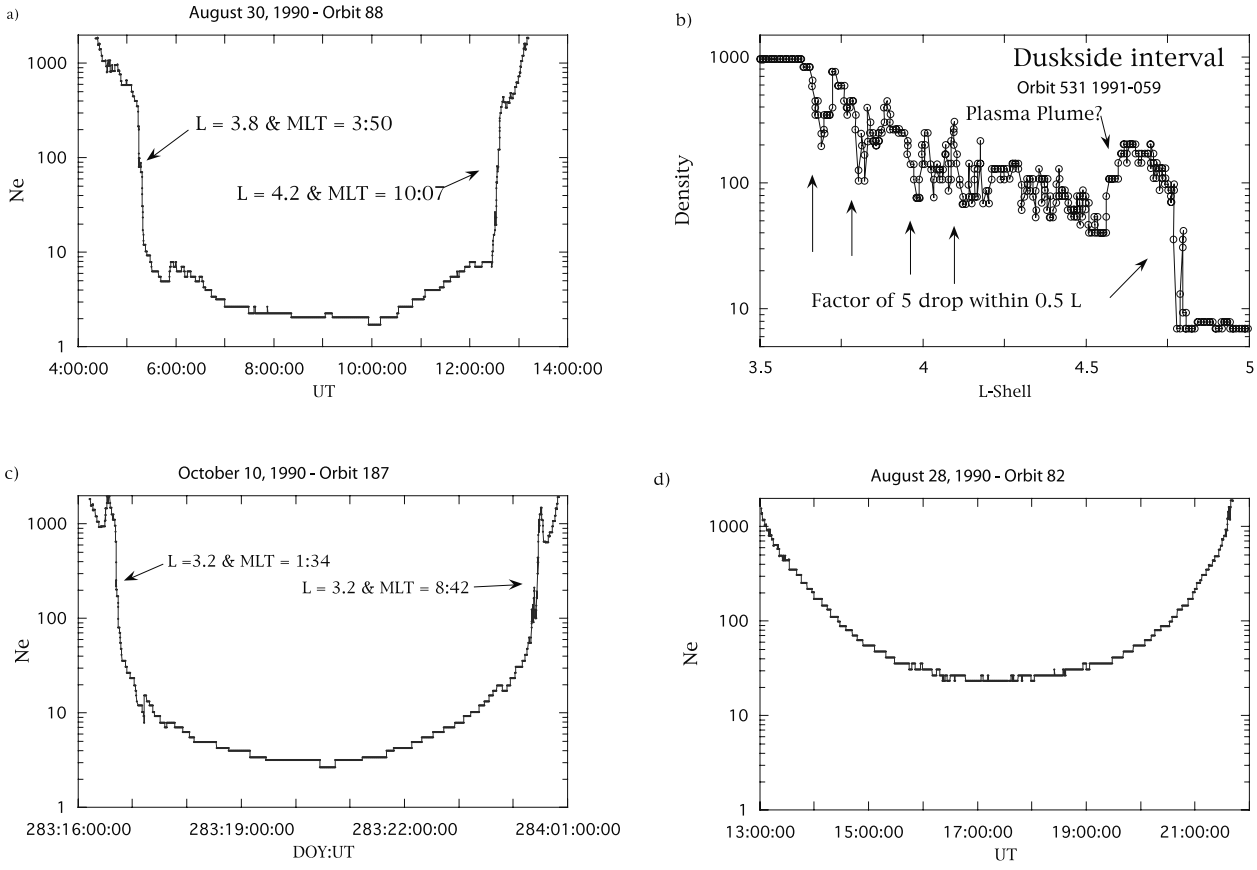

Figure 1. Examples showing the different types of plasmapause typically observed with CRRES. (a) A classic plasmapause profile with sharp, clean density profiles. (b) Orbits with apparently multiple plasmapauses and considerable density structure. (c) Plasmapause crossings accompanied by plasmaspheric density cavities. (d) Extended plasmaspheric intervals when the plasmasphere was beyond the CRRES orbit through apogee.

inbound and outbound orbits) the plasmasphere was not encountered owing to the plasmapause being beyond the apogee of CRRES (see Figure 1d). For the rest of the orbits an innermost density drop was often observed, but it did not have a gradient above our selection criterion of a factor of 5 change within 0.5 L (Figure 3a), essentially had a smooth gradual profile (Figure 3b), or was associated with rapid fluctuations of density that extended in considerable L (Figure 3c). The orbits that had no clear plasmapause were evenly distributed in local time. No clear dependence on LT was found for the different types of density profiles with all three types of profiles occurring during the day and nightside sector. There was a slight Kp dependence found with the "too small gradient" profiles occurring during predominantly quiet conditions whereas the "rapid density fluctuation" profiles occurred during more active conditions.

[11] The locations of the plasmapause in L and magnetic local time (MLT) were binned by a measure of the convection history. We examined several measures of characterizing the geomagnetic activity history including that used by *Carpenter and Anderson* [1992]. Carpenter and Anderson used the maximum *Kp* in the previous 24 hours except for plasmapause crossings in the 0600–0900, 0900–1200, and 1200–1500 LT sectors. For those plasmapauses the *Kp* values for one, two or three immediately preceding 3-hour periods were ignored to attempt to account for the expected delay in plasmapause response to enhanced convection activity on the dayside. We found that the variability of the relationship between *Kp* and Lpp very slightly decreases, and the range of *Kp* levels included increases, by using the maximum *Kp* in the previous 12 hours and not accounting for a delay in response for the dayside observations. We found that the plasmapause can move a significant distance between consecutive 10-hour orbits and that using 12 hours gave a good correlation between plasmapause position and *Kp*. For plasmapause crossings that occurred within the first hour of the 3-hour *Kp* interval, the previous four *Kp* values (12 hours) were examined for the maximum. For plasmapause crossings that occurred in the second or third hour of the *Kp* interval, that *Kp* value and the previous three *Kp* values were examined.

[12] Figure 4 shows the location of the plasmapause as a function of *Kp* for all LT. Though there is a clear trend of decreasing L shell with increasing *Kp*, the scatter is significant. Figure 5 examines how the location of the mean plasmapause varies as a function of LT and *Kp*. The mean Lpp are divided into 2-hour local time sectors and four levels of *Kp* (0–2+, 3, 4, >5). Overlaid onto these figures are the locations of the actual Lpp to give a sense of the variability as well as the standard deviation about the mean

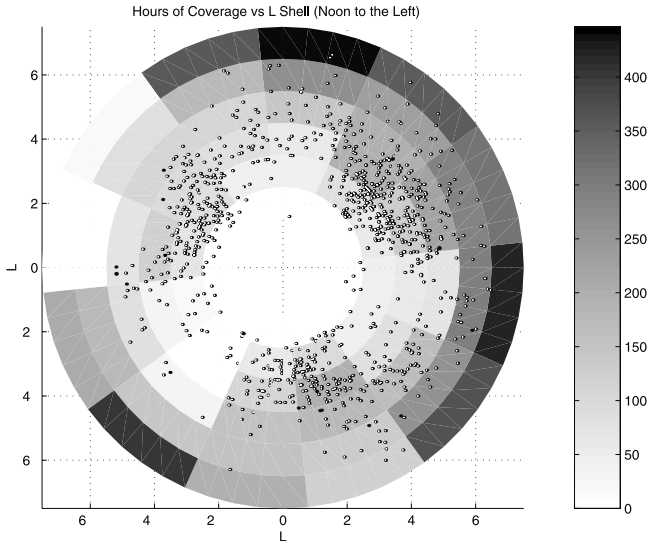

Figure 2. The number of hours of CRRES plasma wave observations in 2-hour by 1 L shell bins shown as a polar plot with noon to the left. The gap in coverage at high L shell near noon is due to the untimely demise of the CRRES mission prior to the line of apsides making a complete rotation about the Earth. The location of each individual plasmapause crossing identified in the CRRES database is superimposed as open circles.

for the different local time bins. If there were less than seven Lpp observations in the bin, no mean value is plotted. These intervals were selected to maximize the resolution in LT and *Kp* but also to assure adequate statistics in each bin. The same trend seen in Figure 4 is seen for the mean plasmapause locations, namely the plasmapause moves closer to the Earth for increasing *Kp* at essentially all local times. However, there is a marked difference in the mean location of the plasmapause around noon compared to that at midnight with the mean plasmapause located closer to the Earth at noon than at midnight. The bottom two panels of Figure 5 show the mean location of the plasmapause as a function of *Kp* and the best fit models to the actual data points. Note that the mean Lpp in the dusk sector essentially overlap as a function of Kp owing to the significant scatter in the location of the Lpp for essentially all levels of activity.

[13] Figure 6 shows the relationship between Lpp and *Kp* for the four local time sectors centered on midnight (2100–0300 LT), dawn (0300–0900 LT), noon (0900–1500 LT), and dusk (1500–2100 LT). The dayside sector shows a lack of plasmapause crossings at L shells >5, whereas in the night sector plasmapauses are observed at large L for low *Kp*. The dusk sector has considerable more scatter than the other local time sectors and shows that the Lpp can be found at essentially any L shell for any $Kp \leq 5$. The best fit equations and correlation coefficients are shown with the figures and in Table 1. Table 1 also shows the uncertainties in the y-intercept and slope and the standard deviation of the L shell values about the best fit line. In addition, Table 1 shows the same fit parameters for the "traditional" local time sectors of 0000–0600 LT, 0600–1200 LT, 1200–1800 LT, and 1800–2400 LT. This information is provided in order to compare to previous work and is discussed in section 4.

[14] The main conclusions that come out of these results is that the plasmasphere is essentially circular for a given level of *Kp*. However, there are three important caveats to this conclusion. (1) The nightside plasmasphere extends 0.5 to 1 L shell farther than the dayside plasmapause for low geomagnetic activity, (2) the dusk sector is highly variable with only a weak dependence on decreasing Lpp for increasing *Kp* levels and (3) significant scatter is seen at all local times with standard deviations of the Lpp position on the order of 0.5 L.

[15] By binning the data into 2-hour local time by 1 L shell bins we can examine the influence of the incomplete orbital coverage on the first result. We examined the number of hours of observations made in each local time bin for L shells >5 and compared that with the occurrence frequency of plasmapause observations (Lpp/hour of data). For the

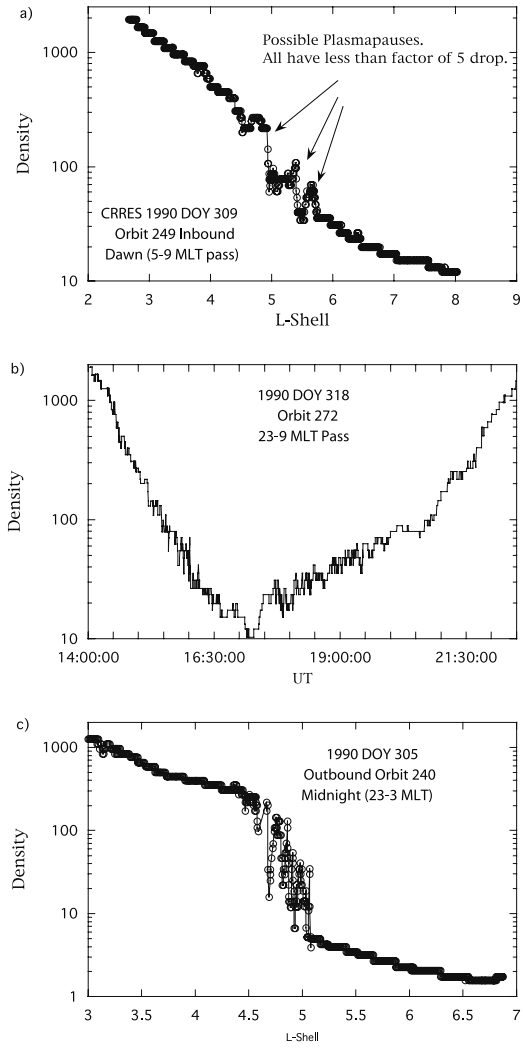

Figure 3. Several examples of orbits that did not have an identifiable plasmapauses are shown. (a) About 40% of these orbits had "plasmapause-like" gradients, but the gradients did not meet our factor of 5 density change within 0.5L. (b) About 20% of these orbits had relatively smoothly varying density profiles and (c) the remaining 40% had highly structured density variability over an extended range of L.

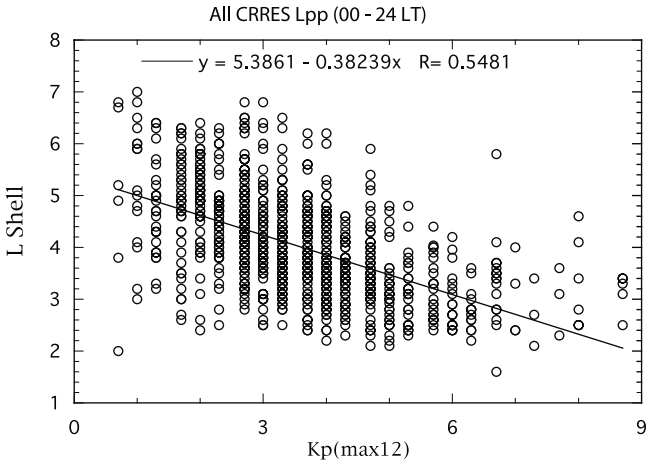

Figure 4. The location of the plasmapause at all local times as a function of *Kp*(max) shows a clear trend of decreasing plasmapause distance with increasing *Kp*, though there is significant scatter.

nightside sector the occurrence frequency ranges from 0.07–0.17 Lpp/hr at L shells between 5 and 6 to 0–0.04 Lpp/hr for L shells >6. Within the dayside sector the occurrence frequency is considerably smaller for both L shell bins. Though the amount of data at these local times and L shells is less than in the nightside sector, there are still hundreds of hours of observations (except in the two local time sectors between 0800–1200 LT where there is only 12 hours of observations beyond L of 6 and <50 hours of data between L of 5 and 6). For the early afternoon sector there is a large amount of data at high L shells though no plasmapause crossings. However, an examination of the intervals that had no Lpp crossings owing to having the plasmapause located beyond apogee found that several of these occurred in the dayside sector. This suggests that the plasmasphere occasionally does exist near geosynchronous orbit on the dayside, however the transition from plasmasphere to trough is not sharp enough to meet our selection criteria of a factor of 5 decrease in density over 0.5 L.

[16] A further examination of the duskside sector shows that the high variability is primarily confined in the 1600–2000 LT sector. This sector shows the most structure beyond the main plasmapause and has a standard deviation in the Lpp location >1 L shell. The plasmapause can be observed essentially at any L shell for *Kp* levels between 0 and 5.

3.2. Plasmapause Location Model

[17] The average location of the plasmapause as a function of *Kp*(max) depends on local time sector. Figure 5 shows that in the dayside sector (between 0900 and 1500 LT) the average location of the plasmapause are located at distances earthward of the plasmapause in the nightside sector (2100–0300 LT). The following relationship gives the location of the plasmapause as determined from the best linear fit to all the Lpp identified by CRRES in all local times.

$$\mathrm{Lpp} = (5.39 \pm 0.072) - (0.382 \pm 0.019)Kp(\max) \quad (\mathrm{R} = 0.5481) \tag{2}$$

The standard deviation of the observations about this line is ≈0.7 L. The standard deviation of the observations can be significantly narrowed by binning the data as a function of LT. Table 1 shows the best fit parameters for the four traditional and the four LT sectors centered on noon, dusk, midnight, and dawn. These later four equations give the best fit to the plasmapause observations as a function of *Kp* and MLT and are shown in the last panel in Figure 5.

4. Discussion

4.1. Summary of Results

[18] The plasmapause position (defined as the innermost steep density gradient) depends on the local time of observation and the recent time history of magnetospheric convection. This study has developed a linear relationship between Lpp and the maximum *Kp* in the previous 12 hours. We found that the data are best described if binned into four local time sectors. The plasmapause location on the dayside (from 0900–1500 LT) is on average ~0.5 to 1 L shell earthward than the plasmapause on the nightside (from 2100–0300 LT). This difference is primarily due to the relative absence of plasmapause crossings beyond L of 5 on the dayside. The variability of the location of the plasmapause is large. The variability is largest for low *Kp* and in the dusk sector for all levels of *Kp*.

4.2. Comparison With Earlier Results

[19] The main previous empirical plasmapause location model was that of *Carpenter and Anderson* [1992]. In that study, 208 plasmapause crossings from ISEE 1 were examined as a function of *Kp* and the linear relationship given in equation (1) was found for the local time sector 0000–1500 LT. The new CRRES results find essentially identical relationship if the data are restricted to the same 0000–1500 LT bin. However, the CRRES plasmapause model results for all local times find that there is a marked difference in plasmapause location between the day and nightside especially for low geomagnetic activity. This difference was not found in the Carpenter and Anderson study. This is primarily due to the limitation of the ISEE database modeling to the 0000–1500 LT sector. However, ISEE plasmapause crossing data were obtained at all local times and displayed in their Figure 7. For the 1200–0000 LT sector where both the ISEE and CRRES data sets have ample data coverage at large L there is very good agreement. Both data sets see only one Lpp located beyond an L of 6 in the 1200–1800 LT sector and a number of Lpp beyond L of 6 in the 1800–0000 LT sector. However, using a 2-hour running average the ISEE plasmapause location is essentially circular with no noon-midnight or dawn-dusk asymmetry.

[20] *Gringauz and Bezrukikh* [1976] using data from the polar orbiting Prognoz-2 satellite also found an asymmetry in the location of the plasmapause in the direction of noon-midnight. However, that study found that the asymmetry was such that the plasmapause was located at higher L at noon than at midnight for quiet geomagnetic activity. The Prognoz-2 was in a 65° inclination orbit with an ~30 Re apogee and therefore crossed the plasmapause four times per orbit (twice at high altitude and twice near perigee at low altitude). The study examined only the high altitude

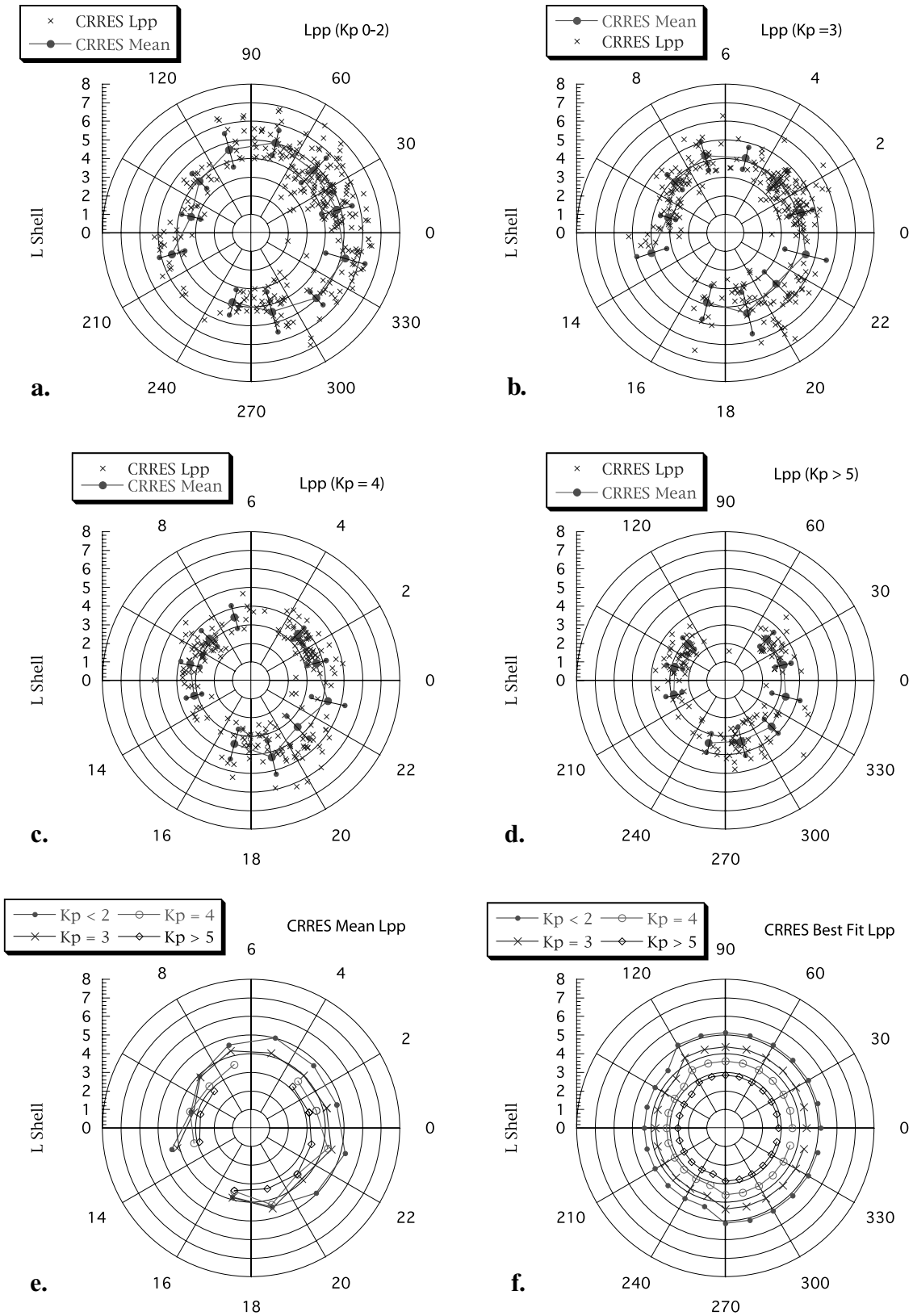

Figure 5. The mean location of the plasmapause in 2-hour local time bins as a function of *Kp*(max) is shown divided into four different *Kp* levels. Note the day-night asymmetry seen for low *Kp* with the dayside plasmapause located on average 1 L shell Earthward than the corresponding nightside average. (e and f) The mean Lpp location and the best fit model for the actual Lpp locations.

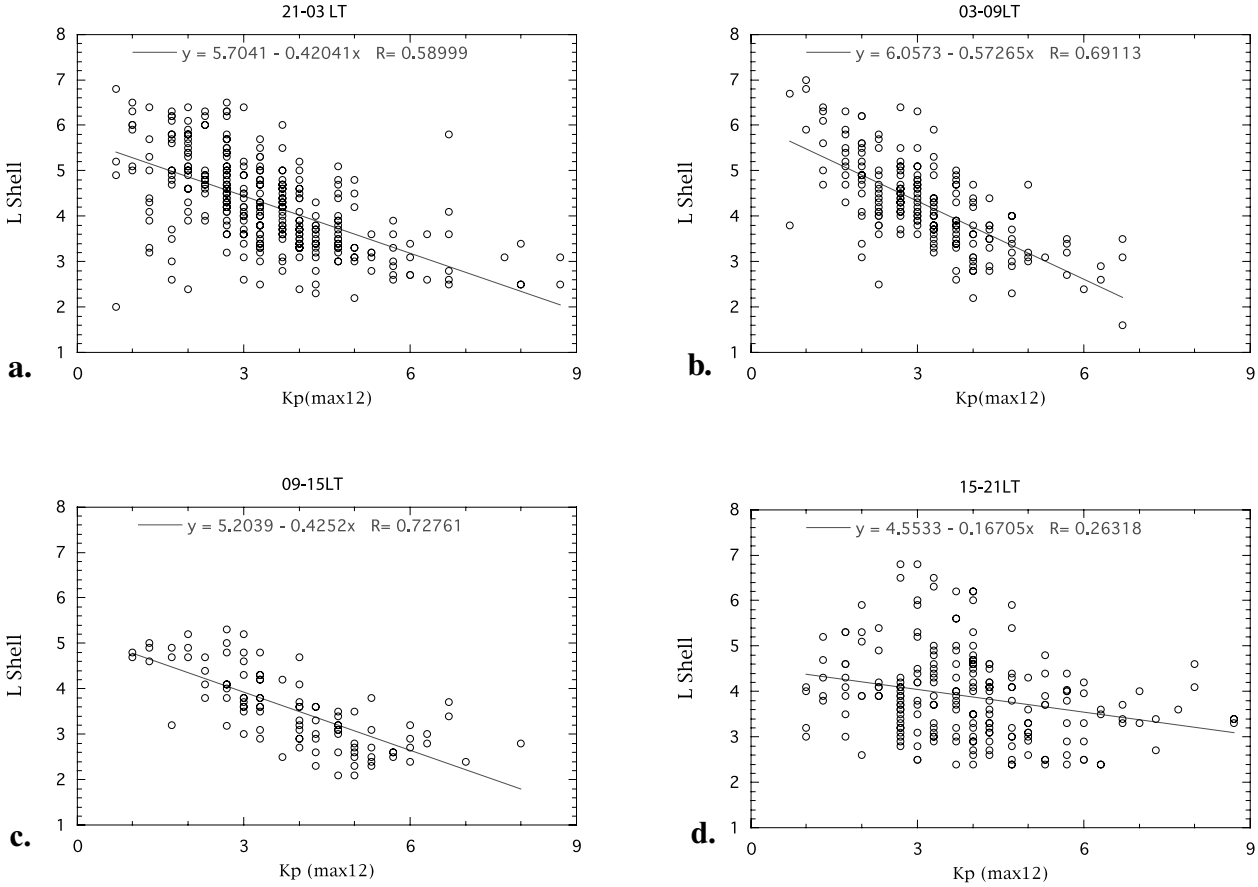

Figure 6. The location of the plasmapause as a function of *Kp* is shown for four different local time sectors centered on (a) midnight, (b) dawn, (c) noon, and (d) dusk. Linear fits are used to develop the plasmapause location model.

crossings for 18 orbits and found that the plasmapause on the dayside was located at considerably higher L than the corresponding nightside plasmapause for quiet activity levels whereas the asymmetry disappears for disturbed conditions. The Prognoz-2 data set show essentially "simultaneous" day and night crossings whereas the CRRES and ISEE databases can only address the average location on the day and night in a statistical sense. No such asymmetry is found even when looking at narrow local time sectors. In this study (and *Carpenter and Anderson* [1992]), the innermost plasmapause was selected. This has the effect of discounting dense plasmaspheric regions that extend beyond the main plasmapause. *Elphic et al*. [1996] showed that during high levels of geomagnetic activity cold plasmaspheric plasma is often seen at geosynchronous orbit in the noon sector. The Prognoz-2 results could reflect the identification of this noon-dusk bulge [*Carpenter*, 1970; *Chappell et al.*, 1970; *Maynard and Chen*, 1975].

[21] The noon-midnight asymmetry found in the CRRES database is primarily due to the lack of Lpp at high L shells in the dayside. Because plasmaspheric plasma was observed occasionally at high L during quiet times in the dayside sector, we suggest that the absence of Lpp at L > 5 on the dayside is partially due to the gradient selection criterion. We required a factor of 5 decrease over a distance of 0.5 L. Our study suggests that sharp gradients can be observed out to geosynchronous orbit on the nightside but not on the dayside. This is consistent with earlier results that found the nightside trough is often an order of magnitude lower density that the dayside trough [e.g., *Chen et al.*, 1976; *Decreau et al.*, 1982; *Sheeley et al.*, 2001]. Therefore sharper gradients between the plasmasphere and the trough should exist at night. This is due to the effect of dayside plasmaspheric refilling creating an asymmetry in the day/night trough densities.

[22] *Horwitz et al.* [1986] examined the location of the low-energy ion transition (LEIT) using DE 1 and 2. The LEIT corresponds to the open/closed convection boundary and hence is thought to track the plasmapause. They found

Table 1. The Linear Best Fit Parameters of the Form Lpp = (A ± σ_A) + (B ± σ_B) Kp

LT Sector	A	B	σ_{Lpp}	σ_A	σ_B	R
0000–2400	5.39	−0.382	0.678	0.072	0.019	0.548
0000–0600	5.70	−0.45	0.689	0.092	0.026	0.659
0600–1200	5.12	−0.400	0.681	0.144	0.039	0.603
1200–1800	4.92	−0.314	0.711	0.190	0.047	0.553
1800–2400	5.25	−0.272	1.03	0.171	0.043	0.379
2100–0300	5.70	−0.420	0.631	0.089	0.031	0.590
0300–0900	6.05	−0.573	0.468	0.138	0.041	0.691
0900–1500	5.20	−0.425	0.330	0.165	0.040	0.728
1500–2100	4.45	−0.167	0.928	0.174	0.0413	0.263

The standard deviation of the individual points about the best fit line is given as σ_{Lpp} and the linear correlation coefficient is given as R.

in the afternoon/evening sector (1500–2400 LT) a relationship between the LEIT and *Kp* (where the 3-hour *Kp* value was used at the time of LEIT observation). The LEIT-L shell relationship found was

$$L = 7.89 - 0.78Kp \quad (3)$$

This has a y-intercept 2.5L higher then the corresponding CRRES result in the same local time sector and a slope nearly 3 times as large. The orbit of CRRES induces a bias in the CRRES results by not sampling at L shells generally higher the 7. However, the main reason for the different results is that the LEIT was not observed below L of 5 for $Kp < 2$. This implies that the LEIT does not correspond to the innermost sharp density gradient except during active conditions. This was suggested by *Horwitz et al.* [1986], who proposed that the LEIT was a more sensitive signature of the open/closed convection boundary rather than the sharp density gradient. This study confirms this and shows that the instantaneous open/closed convection boundary is most often far from the plasmapause as defined by a sharp density gradient.

4.3. Plasmapause Location Variability

[23] There is significant variability in the location of the plasmapause for a given level of *Kp*. This is in part due to the imperfect characterization of convection history by using a single *Kp* value as well as the possible LT and L shell dependent response of the plasmapause to changes in geomagnetic activity [e.g., *Carpenter et al.*, 1993]. The variability is most pronounced in the dusk sector and for low levels of geomagnetic activity. This latter result is consistent with the geosynchronous orbit observations that the local time of appearance of plasmaspheric plasma is highly variable for $Kp \leq 2$, whereas there is a systematic relationship between LT and *Kp* for *Kp* levels over 2 [*Moldwin et al.*, 1994].

[24] Recent IMAGE EUV images show that the EUV plasmapause often shows a duskside bulge and drainage plume as well as surface "biteouts" and shoulders [*Sandel et al.*, 2001]. These surface features generally have a radial extent comparable to the variability seen in this CRRES study. In addition, IMAGE has shown that there is often significant radial structure limited to a narrow MLT sector. This structure often corotates. Therefore part of the variability seen in the average plasmapause location is due to these small-scale surface features that can give rise to variations on the order of an L shell.

5. Conclusions

[25] This study has developed a model of the location of the plasmapause using over 1000 orbits of CRRES plasma wave data valid at all local times. The data show that the average plasmapause is essentially circular, varying linearly with *Kp*. However, especially during quiet geomagnetic conditions there is a slight asymmetry in the noon-midnight direction with the plasmapause located at higher L shells in the night sector. The CRRES empirical model also contains the standard deviation of the measured plasmapause locations compared with the linear best fit locations. The standard deviation is also a function of *Kp* with the variability of the plasmapause location being typically a factor of 2 greater at low *Kp* than high *Kp*. The difference in results from the *Gringauz and Bezrukikh* [1976] study, maybe owing to the large average variability of the plasmapause location for low geomagnetic activity levels and/or owing to our large density gradient requirement.

[26] This new empirical and analytical plasmapause model with a measure of the variability of the plasmapause location can be incorporated into numerical models and can be used in interpreting global plasmaspheric images. The extension of the model to the dusk and nightside is an improvement over previous empirical models with more limited local time ranges. In addition, the factor of 5 increase in the number of plasmapause crossings allowed a more meaningful examination of the plasmapause with respect to geomagnetic activity levels and local time. The standard deviation of the data about the linear best fit plasmapause is given in order to describe the large variability in the location of the plasmapause particularly for low geomagnetic activity levels. This model can be combined with the CRRES density model of the plasmasphere and trough [e.g., *Sheeley et al.*, 2001] in order to develop a complete density model of the inner magnetosphere.

[27] **Acknowledgments.** This work was supported by NASA grants NAGW-5153 and NAG5-4897 and a REU supplement to NSF grant ATM-9628708.

[28] Lou-Chuang Lee and Chin S. Lin thank James Horowitz and Dennis L. Gallagher for their assistance in evaluating this paper.

References

Anderson, R. R., D. A. Gurnett, and D. L. Odem, CRRES plasma wave experiment, *J. Spacecr. Rockets*, *29*, 570, 1992.

Borovsky, J. E., M. F. Thomsen, and D. J. McComas, The superdense plasma sheet: Plasmaspheric origin, solar wind origin, or ionospheric origin?, *J. Geophys. Res.*, *102*, 22,089, 1997.

Carpenter, D. L., and R. R. Anderson, An ISEE/whistler model of equatorial electron density in the magnetosphere, *J. Geophys. Res.*, *97*, 1097, 1992.

Carpenter, D. L., B. L. Giles, C. R. Chappell, P. M. E. Décréau, R. R. Anderson, A. M. Persoon, A. J. Smith, Y. Corcuff, and P. Canu, Plasmasphere dynamics in the duskside bulge region: A new look at an old topic, *J. Geophys. Res.*, *98*, 19,243, 1993.

Carpenter, D. L., R. R. Anderson, W. Calvert, and M. B. Moldwin, CRRES observations of density cavities inside the plasmasphere, *J. Geophys. Res.*, *105*, 23,323, 2000.

Chappell, C. R., K. K. Harris, and G. W. Sharp, The morphology of the bulge region of the plasmasphere, *J. Geophys. Res.*, *75*, 3848, 1970.

Chappell, C. R., K. K. Harris, and G. W. Sharp, The dayside of the plasmasphere, *J. Geophys. Res.*, *76*, 7632, 1971.

Chen, A. J., J. M. Grebowsky, and K. Marubashi, Diurnal variation of thermal plasma in the plasmasphere, *Planet. Space Sci.*, *24*, 765, 1976.

Decreau, P. M. E., C. Beghin, and M. Parrot, Global characteristics of the cold plasma in the equatorial plasmapause region as deduced from the GEOS 1 mutual impedance probe, *J. Geophys. Res.*, *87*, 695, 1982.

Doe, R. A., M. B. Moldwin, and M. Mendillo, Plasmapause morphology determined from an empirical ionospheric convection model, *J. Geophys. Res.*, *97*, 1151, 1992.

Elphic, R. C., M. F. Thomsen, and J. E. Borovsky, The fate of the outer plasmasphere, *Geophys. Res. Lett.*, *24*, 365, 1997.

Gallagher, D. L., P. D. Craven, and R. H. Comfort, Global Core Plasma model, *J. Geophs. Res.*, *105*, 18,819, 2000.

Gary, S. P., M. B. Moldwin, M. F. Thomsen, and D. Winske, Hot proton anisotropies and cool proton temperatures in the outer magnetosphere, *J. Geophys. Res.*, *99*, 23,604, 1994.

Higel, B., and L. Wu, Electron density and plasmapause characteristics at 6.6 RE: A statistical study of the GEOS 2 relaxation sounder data, *J. Geophys. Res.*, *89*, 1583, 1984.

Horwitz, J. L., S. Menteer, J. Turnley, J. L. Burch, J. D. Winningham, C. R. Chappell, J. D. Craven, L. A. Frank, and D. W. Slater, Plasma boundaries in the inner magnetosphere, *J. Geophys. Res.*, *91*, 8861, 1986.

Kozyra, J. U., V. K. Jordanova, R. B. Horne, and R. M. Thorne, Interaction

of ring current and radiation belt protons with ducted plasmaspheric hiss, 2, Time evolution and distribution function, *J. Geophys. Res.*, *100*, 21,911, 1995.

Lambour, R. L., L. A. Weiss, R. C. Elphic, and M. F. Thomsen, Global modeling of the plasmasphere following storm sudden commencements, *J. Geophys. Res.*, *102*, 24,351, 1997.

LeDocq, M. J., D. A. Gurnett, and R. R. Anderson, Electron number density fluctuations near the plasmapause observed by the CRRES spacecraft, *J. Geophys. Res.*, *99*, 23,661, 1994.

Lemaire, J., Steady state plasmapause positions deduced from McIlwain's electric field models, *J. Atmos. Terr. Physics*, *38*, 1041, 1976.

Lemaire, J., and K. I. Gringauz, *The Earth*'s *Plasmapause*, 350 pp., Cambridge Univ. Press, New York, 1998.

Maynard, N. C., and A. J. Chen, Isolated cold plasma regions: Observations and their relation to possible production mechanisms, *J. Geophys. Res.*, *80*, 1009, 1975.

Maynard, N. C., and J. M. Grebowsky, The plasmapause revisited, *J. Geophys. Res.*, *82*, 1591, 1977.

Maynard, N. C., W. F. Denig, and W. Burke, Mapping ionospheric convection patterns to the magnetosphere, *J. Geophys. Res.*, *100*, 1713, 1995.

Moldwin, M. B., M. F. Thomsen, S. J. Bame, D. J. McComas, and K. R. Moore, An examination of the structure and dynamics of the outer plasmasphere using multiple geosynchronous satellites, *J. Geophys. Res.*, *99*, 11,475, 1994.

Sandel, B. R., R. A. King, W. T. Forrester, D. L. Gallagher, A. L. Broadfoot, and C. C. Curtis, Initial results from the IMAGE Extreme Ultraviolet Imager, *Geophys. Res. Lett.*, *28*, 1439, 2001.

Sheeley, B. W., M. B. Moldwin, H. K. Rassoul, and R. R. Anderson, An empirical plasmasphere and trough density model: CRRES Observations, *J. Geophys. Res.*, *106*, 25,631, 2001.

Takahashi, K., and B. J. Anderson, Distribution of ULF energy (f < 80 mHz) in the inner magnetosphere: A statistical analysis of AMPTE CCE magnetic field data, *J. Geophys. Res.*, *97*, 10,751, 1992.

Thorne, R. M., and R. B. Horne, The contribution of ion-cyclotron waves to electron heating and SAR-arc excitiation near the storm-time plasmapause, *Geophys. Res. Lett.*, *19*, 419, 1992.

Webb, D., and D. Orr, Spectral studies of geomagnetic pulsations with periods between 20 and 120 sec and their relationship to the plasmapause region, *Planet Space Sci.*, *23*, 1551, 1975a.

Webb, D., and D. Orr, Statistical studies of geomagnetic pulsations with periods between 20 and 120 sec and their relationship to the plasmapause region, *Planet Space Sci.*, *23*, 1169, 1975b.

Wilson, G. R., J. L. Horwitz, and J. Lin, A semikinetic model for early stage plasmasphere refilling, 1, Effects of coulomb collisions, *J. Geophys. Res.*, *97*, 1109, 1992.

Young, D. T., S. Perraut, A. Roux, C. deVilledary, R. Gendrin, A. Korth, G. Kremser, and D. Jones, Wave-particle interactions near Ω_{He+} observed on GEOS 1 and 2, 1, Propagation of ion cyclotron waves in He^+-rich plasma, *J. Geophys. Res.*, *86*, 6755–6772, 1981.

R. Amin, L. Downward, and H. K. Rassoul, Department of Physics and Space Sciences, Florida Institute of Technology, Melbourne, FL 32901, USA. (ramin@phys.ufl.edu; lmd@physics.ucsc.edu; rassoul@Galileo.pss.fit.edu)

R. R. Anderson, Department of Physics and Astronomy, University of Iowa, 615 Van Allen Hall, Iowa City, IA 52242-1479, USA.

M. B. Moldwin, Department of Earth and Space Sciences, University of California, Los Angeles, 3845 Slichter Hall, Los Angeles, CA 90095-1567, USA. (mmoldwin@igpp.ucla.edu)